Generation of $J_c(H_e)$ hysteresis curves for granular $YBa_2Cu_3O_{7-\delta}$ superconductors*

E. Altshuler, J. Musa, J. Barroso, A.R.R. Papa and V. Venegas

Superconductivity Laboratory, IMRE, University of Havana, 10400 Havana, Cuba

The experimental hysteretic behaviour of the transport critical current density $J_c(H_e)$ observed in granular $YBa_2Cu_3O_{7-\delta}$ has been compared with the analogous theoretical curves resulting from a well known model based on the effect of flux trapped by the superconducting grains at the intergranular junctions. The magnetization of the grains was calculated for different values of maximum applied field H_m using the Bean model; at the same time the statistical distribution of the qualities of the junctions was taken into account. This approach was seen to predict the evolution of hysteretic $J_c(H_e)$ curves for different values of H_m with reasonable accuracy.

Keywords: high T_c superconductivity; Y-Ba-Cu-O; critical currents; weak links

Although the dependence of the transport critical current density J_c on the external field has been extensively studied in ceramic superconductors for increasing fields, much less work has been done on the hysteretic (decreasing field) J_c *versus* H curves[1-5].

Evetts and Glowacki[2] gave a qualitative explanation of the hysteretic J_c *versus* H behaviour by analysing the effect that the flux trapped by the superconducting grains, or by persistent loops in the wake link network, produces on the weak links between grains, which are supposed to control the transport critical current density in these materials. In this picture, a minimum in the effective field at the junctions provokes a maximum in the decreasing field J_c *versus* H_e characteristic. However, only a few attempts have been made to determine a quantitative approach to the problem. In reference 3, for example, a hysteretic J_c *versus* H_e curve is generated, based on a model in which flux is trapped by persistent loops in the weak link network (WLN) instead of the grains, but fits to experimental data are not shown. Other work (see, for example, reference 6) concentrates on the 'internal field' acting at the weak links in a way akin to the qualitative Evetts and Glowacki model. Navarro and Campbell[7], however, calculated the 'intergranular' field of a medium of spherical grains, obtaining no minimum for either an increasing or a decreasing field, which is interpreted by the authors as strong evidence against the Evetts and Glowacki picture. In this paper, we work through the basic idea of the model given in reference 2 quantitatively and compare the results with experiments for the case of an $YBa_2Cu_3O_{7-\delta}$ ceramic sample.

* Paper presented at the conference 'Critical Currents in High T_c Superconductors', 22 – 24 April 1992, Vienna, Austria

0011 – 2275/93/030308 – 06

Theory

Fitting formula

If we regard the ceramic superconductor as a random assembly of type II superconducting grains interconnected by S-I-S Josephson junctions[8], the following formula[9] can be used to fit the dependence of J_c on the external magnetic field, when it is increased after zero field cooling (ZFC)

$$\frac{J_c(H_e)}{J_c(0)} = \int_{H_o(\min)}^{H_o(\max)} \Omega(H_o) \left| \frac{\sin \pi H_e/H_o}{\pi H_e/H_o} \right| dH_o \qquad (1)$$

Here, $J_c(0)$ is the critical current density at $H_e = 0$ and $\Omega(H_o)$ is a statistical distribution of H_o normalized to unity, where H_o is the field value for which the first flux quantum penetrates a Josephson junction. Any experimental $J_c(H_e)/J_c(0)$ dependence can be fitted by formula (1) if an appropriate distribution $\Omega(H_o)$ is chosen.

Let us assume that the magnetic field has been increased to a value $H_m > H_{c1g}$, where H_{c1g} is the first critical field of the grains, so they have been partially penetrated by the field following some critical state model. Then, when H_e is decreased, the junctions 'feel' an effective field $\boldsymbol{H}_{eff}$, which is roughly the resultant value of the vectorial sum of the external field plus the field at the junctions associated to grain magnetization, $\boldsymbol{H}_{gj}$.

If one assumes that the grains are thin slabs with their long axis parallel to the external field[10] and that the width of the Josephson junctions is much smaller than that of the grains (see *Figure 1*), one can propose the

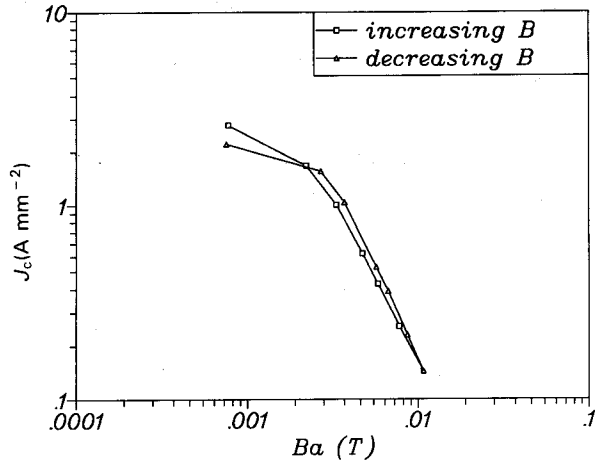

Figure 11 Typical magnetic field dependence of critical current density of plasma sprayed Y-Ba-Cu-O on nickel, measured at 60 K

Acknowledgements

This work was supported by the Commission of the European Community within the Brite-EuRam programme under Contract BREU-0124.

References

1 **McPherson, R.** *Surface Coatings Technol* (1989) **39/40** 173
2 **Elam, W.T., Kirkland, J.P., Neiser, R.A., Skelton, E.F. *et al.*** *Adv Ceram Mater* (1987) **2** (3B) 411
3 **Kirkland, J.P., Neiser, R.A., Herman, H., Elam, W.T. *et al.*** *Adv Ceram Mater* (1987) **2** (3B) 401
4 **Cuomo, J.J., Guarnierie, C.R., Shivashankar, S.A., Roy, R.A. *et al.*** *Adv Ceram Mater* (1987) **2** (3B) 422
5 **Karthikeyan, J., Paithankar, A.S., Sreekumar, K.P., Venkatramani, N. *et al.*** *Cryogenics* (1989) **29** 915
6 **Chu, W.F. and Rohr, F.J.** *Physica C* (1988) **153/155** 802
7 **Tachikawa, K., Watanabe, I., Kosuge, S., Kabasawa, M. *et al.*** *Appl Phys Lett* (1988) **52** 1011
8 **Konaka, T., Sankawa, I., Matsuura, T., Higashi, T. *et al.*** *Jpn J Appl Phys* (1988) **26** L1092
9 **Sankawa, I., Konaka, T., Matsuura, T. and Ishihara, K.** *Jpn J Appl Phys* (1988) **26** L1083
10 **Rohr, S., Eckart, G., Bächer, I., Schläfer, U. *et al.*** *Mod Phys Lett B* (1990) **4** 717
11 **Lacombe, J., Danroc, J. and Kurka, G.** *J Less Common Met* (1990) **164/165** 509
12 **Bouanani, A.M., Suryanarayanan, R., Brun, G., Gorochov, O. *et al.*** *J Less Common Met* (1990) **164/165** 493
13 **Karthikeyan, J., Sreekumar, K.P., Kurup, M.B., Patil, D.S. *et al.*** *J Phys D: Appl Phys* (1988) **21** 1246
14 **Mori, N., Itoi, Y. and Okuyama, M.** *Jpn J Appl Phys* (1989) **28** L237
15 **Lisowski, W., Hemmes, H., Jäger, D., van Silfhout, A. *et al.*** *High Temperature Superconductor Thin Films: Proc ICAM 91* (Ed Correra, E.) North Holland, Amsterdam (1992) 853
16 **Lisowski, W., Hemmes, H., Jäger, D., Stöver, D. *et al.*** *Appl Surface Sci* (1992) **62** 13
17 **Tinkham, M.** *Helv Phys Acta* (1988) **61** 443
18 **Mannhart, J., Chaudhari, P., Dimos, D., Tsuei, C.C. *et al.*** *Phys Rev Lett* (1988) **21** 2476

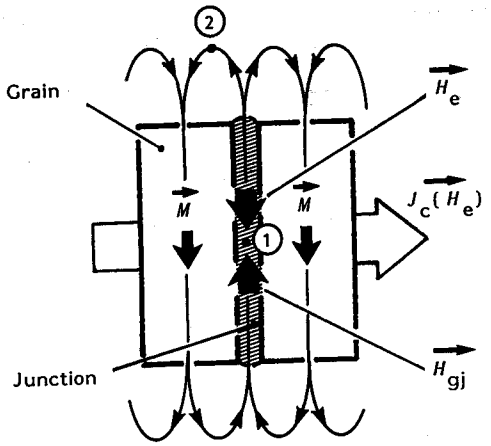

Figure 1 Assumed geometry for calculating the effective field at the junctions

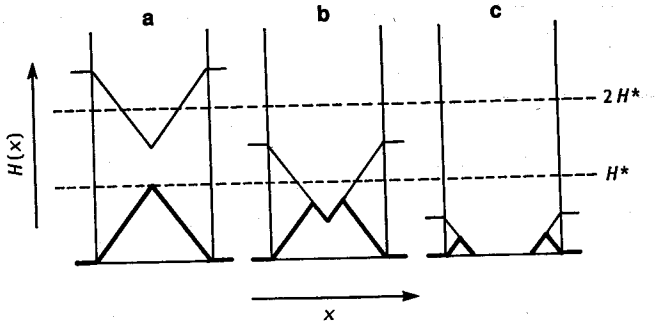

Figure 2 $H(x)$ profiles when H_e decreases from $H_e = H_m$ (lighter lines) to $H_e = 0$ (bold lines) calculated using the Bean model for: (a) $H_m \geq 2H^*$; (b) $2H^* \geq H_m \geq H^*$; (c) $H^* \geq H_m \geq 0$

following expression for the magnitude of $\boldsymbol{H}_{\text{eff}}$ between adjacent grains

$$H_{\text{eff}} = H_e - H_{gj} \tag{2}$$

Since there are no physical grounds to suppose that the distribution of 'junction quality' $\Omega(H_o)$ changes when H_e is decreased, we can substitute H_e in formula (1) by H_{eff} given by formula (2) to obtain the dependence $J_c(H_e)$ in the decreasing field regime

$$\frac{J_c(H_e)}{J_c(\text{peak})} = \int_{H_o(\min)}^{H_o(\max)} \Omega(H_o) \left| \frac{\sin \pi H_{\text{eff}}/H_o}{\pi H_{\text{eff}}/H_o} \right| dH_o \tag{3}$$

Here, we have normalized the critical current density to its value at the peak of the returning dependence, J_c(peak), while $\Omega(H_o)$ is normalized to unity. This means that formula (3) contains no information relative to the depression of J_c(peak) below $J_c(0)$ for experimentally observed increasing values of H_m[2,5]. This phenomenon can be explained qualitatively with the help of *Figure 1*. Despite the fact that H_{eff} is given by expression (2) in regions such as 1, there are zones such as 2 in which H_e is never compensated by the field associated with grain magnetization; on the contrary, the effective field always increases as H_m does. Then, if we assume that $J_c(H_e)$ is affected by the effective field at both regions due to its percolative character, its maximum value will fall below $J_c(0)$ as H_m increases.

Calculation of H_{gj}

To obtain expressions for H_{gj}, we first determined the magnetization M of the grains for decreasing external fields as a function of the maximum applied field H_m.

We calculated the evolution of $M(H_e, H_m)$ from $H_e = H_m$ (applied in ZFC conditions) to $H_e = 0$ for the case $H_{c1g} \ll H^*$ using the 'conventional' formulation of the Bean model[11]. The geometry of the grains and their orientation relative to the external field were supposed to fulfil the conditions depicted in *Figure 1*.

For convenience, we worked in three qualitatively different regions of H_m and split the highest H_m region into two ranges of H_e. The results (geometrically illustrated in *Figure 2*) are as follows.

If $H_m \geq 2H^*$:

$$M = -H_e + H_m - H^*/2 - (H_m - H_e)^2/4H^* \tag{4}$$

when $H_m \geq H_e \geq H_m - 2H^*$

$$M = H^*/2 \tag{5}$$

when $H_m - 2H^* \geq H_e \geq 0$

If $2H^* \geq H_m \geq H^*$:

$$M = -H_e + H_m - H^*/2 - (H_m - H_e)^2/4H^* \tag{6}$$

If $H^* \geq H_m \geq 0$:

$$M = H^*/2 + [(H_m + H_e)^2 - (2H^* - H_m + H_e)(2H^* + 3H_e + H_m)]/8H^* \tag{7}$$

$M(H_e, H_m)$ is related to the 'field profile' $H(x)$ shown in *Figure 2* via $M = \langle H(x) \rangle - H_e$. Curiously, although (4) and (5) match the expressions given in reference 12 well, (6) and (7) were not found in the available literature.

The effect of magnetization of the grains at the junctions is then given by

$$H_{gj} = GM(H_e, H_m) \tag{8}$$

where the magnetization is described by Equations (4)–(7) and G is a geometrical factor roughly estimated to be 10^{-1} (see Appendix).

The case in which H_{c1g} is not negligible compared to H^* requires modification of Equations (4)–(8) since it is necessary to take into account not only the volume magnetization (calculated using the Bean model), but also that associated with surface currents[6,13]. This case will not be considered here.

Experimental details

Sample preparation

We prepared sample 1 using a liquid solution solidification technique, following the main steps described in

reference 14. Stoichiometric amounts of Y_2O_3, CuO and $Ba(CH_3COO)_2$ were dissolved in HNO_3, HNO_3 and H_2O, respectively. After mixing the three solutions, we added an aqueous solution of citric acid plus 100 ml of ethylene glycol (5% v/v). We then heated the system until a polymeric resin containing Y, Cu and Ba cations in the desired proportions was obtained. The resin was then heat treated at 500°C for 15 h to remove the organic components. The resulting material was a grey, very fine powder aggregate which was subsequently treated at 840°C for 16 h, pressed into pellets at 1.1 t cm^{-2} and sintered at 920°C for 16 h, followed by a 1°C min^{-1} cooling to room temperature in flowing oxygen. From the pellets we then cut bars of dimensions $10 \times 1 \times 0.5$ mm^3, which were suitable for four-probe measurements.

$J_c(H_m, 0)$ versus H_m curves

An external field H_m was applied in ZFC conditions perpendicular to the current flow along the longest axis of the samples and then decreased to zero, whereupon the critical current density was measured via the four-probe technique using a 10^{-5} V cm^{-1} criterion. The entire process was performed for each value of H_m, having first erased the magnetic history of the previous measurement by taking the sample outside the Dewar for a few seconds in order to exceed the critical temperature.

The resultant $J_c(H_m, 0)$ *versus* H_m dependence was used to obtain values of H_{c1g} and H^*, following the method described in reference 13 (see below).

$J_c(H_e)$ curves

First, a J_c *versus* H_e curve was obtained by increasing the external field from zero to H_m, in which the sample was kept for a few seconds. A second curve was then obtained by decreasing the magnetic field from H_m to zero. The whole process was repeated for each value of H_m, having first erased the magnetic history of the sample. The duration of the field sweeps for the different H_m values was kept approximately constant to avoid artefacts due to flux creep. The relative orientation of the external field as well as the method for measuring J_c correspond to those described above.

Results and discussion

Figure 3 shows the $J_c(0, H_m)$ *versus* H_m characteristic obtained. Following the analysis given in reference 13, $H_{c1g} \approx 80$ A m^{-1} is the statistical lower limit of the first critical field of the grains. On the other hand, we obtained $H^* \approx 2786$ A m^{-1} by introducing H_{c1g} and H_s extracted from *Figure 3* into the equation $H_s = H_{c1g} + 2H^*$ (reference 13). Both values showed good agreement with those determined from the *M versus H* loops obtained using vibrating sample magnetometry[15]. It should be stressed that this very low value of H_{c1g} is quite atypical of high T_c ceramic grains, for which the order of magnitude of this term is generally accepted to be 8000 A m^{-1} (see reference 16). However, when compared to other samples, the $J_c(H_e)$ behaviour of our sample does seem to be representative of $YBa_2Cu_3O_{7-\delta}$ ceramics.

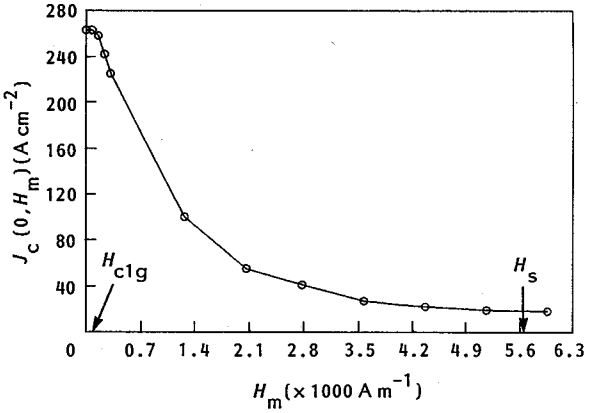

Figure 3 $J_c(0, H_m)$ *versus* H_m experimental characteristic

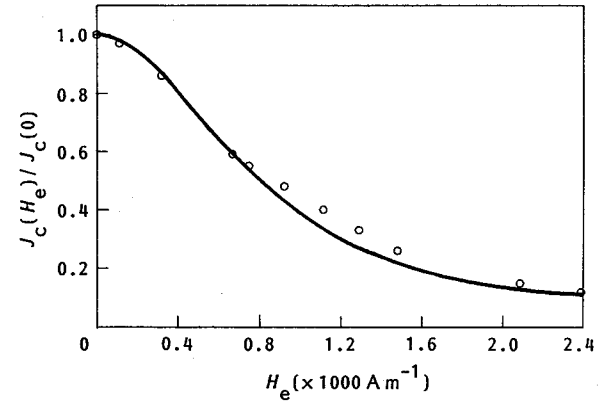

Figure 4 Experimental and theoretical $J_c(H_e)$ characteristics for the increasing-field regime

Figure 4 shows the experimental values of the $J_c(H_e)/J_c(0)$ dependence for the increasing-field regime ('virgin curve'), as well as the fit made following formula (1), with a skewed triangular distribution $\Omega(H_o)$ described by H_o(minimum) = 400 A m^{-1}, H_o(peak) = 1114 A m^{-1} and H_o(maximum) = 3980 A m^{-1}.

Figure 5 shows the decreasing-field ('returning') $J_c(H_e)/J_c$(peak) experimental values for $H_m = 955$ A m^{-1} (*Figure 5a*), $H_m = 1590$ A m^{-1} (*Figure 5b*), $H_m = 4776$ A m^{-1} (*Figure 5c*) and $H_m = 6368$ A m^{-1} (*Figure 5d*), along with the theoretical curves generated using the formulae given above.

The *modus operandi* for the fit of a decreasing-field $J_c(H_e)$ dependence corresponding to a given H_m value was as follows. First, we chose the appropriate expression for $M(H_e, H_m)$ from Equations (4)–(7), as our sample fulfils the condition $H_{c1g} \ll H^*$. Then, the formula for H_{gj} with an initial geometrical factor of 0.1 was inserted into Equations (2) and (3). A theoretical $J_c(H_e)$ curve was then generated following Equation (3) with the same distribution $\Omega(H_o)$ selected to fit the 'virgin' dependence, as noted earlier. This invariability of $\Omega(H_o)$ represents a strong mathematical constraint for fitting the decreasing-field experimental depen-

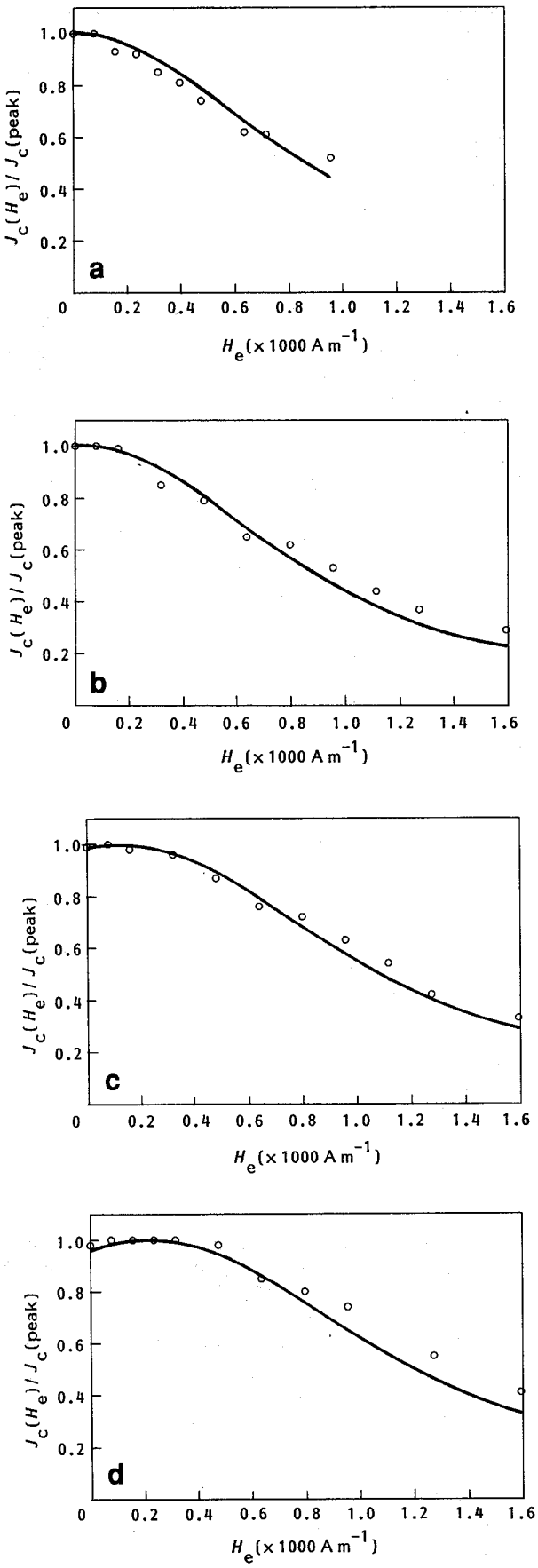

Figure 5 Experimental and theoretical $J_c(H_e)$ characteristics when external field decreases from: (a) H_m = 955 A m^{-1}; (b) H_m = 1590 A m^{-1}; (c) H_m = 4776 A m^{-1}; (d) H_m = 6369 A m^{-1}

dences. Having compared the theoretical $J_c(H_e)$ curve for $G = 0.1$ with the experimental data, the geometrical factor was altered to obtain the best fit by successive approximations. From a geometrical point of view, G 'moves' along the whole bell-shaped characteristic parallel to the H_e axis. The best fit was selected 'by eye'.

The experimental points shown in *Figures 5a* and *b* were fitted using Equation (7) for the magnetization. We selected G 0.16 for the fit, which is close to the theoretical value predicted above. The experimental absence of maxima is also present in the theoretical curves.

Figure 5c displays the fit made with $M(H_e, H_m)$ given by Equation (6) with $G = 0.16$. The appearance of a maximum in the measured curve is predicted by the theoretical model.

We used Equations (4) and (5) for the magnetization in the theoretical fit shown in *Figure 5d*. The geometrical factor was taken as $G = 0.16$, as in the former cases. It should be noticed that the experimental 'shift' in the position of the maximum with respect to *Figure 5c* is predicted by the theory with reasonable accuracy. However, the theoretical curve is somewhat narrower than the experimental dependence, a trend which is more pronounced for fields above 900 A m^{-1}. This fact could be explained if we take into account the statistical character of H_{c1g} and H^*. For example, as H_m increases, the highest H_{c1g} grains begin to trap flux, which 'broadens' the statistical distribution of grains accounting for hysteretic effects. This would presumably broaden the experimental decreasing field $J_c(H_e)$ characteristic as well.

It is remarkable that a single value of the geometrical factor satisfies the fits for the three H_m ranges: variations in G could be expected since, for high values of H_m, the decreasing-field $H(x)$ is 'concentrated' at the centre of the grains, while it 'moves' near the surface for low values of H_m.

The analogous fits we have performed on other $YBa_2Cu_3O_{7-\delta}$ samples (with the necessary adjustments for non-negligible H_{c1g}) are roughly coherent with the one described here: both the maximum shift with H_m and the general shape of the curves are predicted by the model.

Finally we would like to point out some further limitations of the fitting formulae proposed in this work. For very large maximum applied fields (i.e. $H_m \gg 16 \times 10^3$ A m^{-1}), Equations (4)–(7) are no longer valid, since magnetization of the grains does not follow the Bean model. This is clearly demonstrated by *M versus* H_e d.c. loops[15]. The self-field associated with the transport currents is another factor tending to cause deviation of both the virgin and the returning $J_c(H_e)$ curves from the shape predicted by Equations (1) and (3): the self-field is stronger at the regions of the curves with the largest J_c values, thus tending to depress those regions and hence broaden the whole $J_c(H_e)$ characteristic. Even within the low H_m region, there are specific ceramic samples which are very difficult to fit using the formulae given here. Such samples usually present extremely wide returning $J_c(H_e)$ curves combined with high rates of intragranular flux creep or with a lack of repeatability in the measurements of the critical current density (see, for example, reference 17).

Conclusions

We have compared experimental results with decreasing-field $J_c(H_e)$ curves resulting from a model originally described by Evetts and Glowacki[2] in a qualitative fashion, which was complemented by flux trapping calculations and statistical modelling of the grain–junction 'ensemble'.

The model predicts with reasonable accuracy the existence of a peak in the decreasing-field $J_c(H_c)$ characteristics, as well as its shift to higher values of external field as the maximum applied field H_m is increased. On the other hand, quite good agreement was observed between the experimental and theoretical characteristics, although some differences appeared for high values of H_m.

These results have two main implications. First, the Bean model describes quite accurately the low field (i.e. $H_m < 16$ kA m^{-1}) evolution of magnetization for grains of our material, relative to its magnetic history.

Second, our results imply that the simple model used for the grain–junction ensemble[9], as well as the simplified geometry assumed, fits the experimental results, although certain factors such as the self-field associated with the transport current were not taken into account.

The geometrical factor affecting the flux-line distribution at the intergranular junctions appeared to be quite independent of the external field and H_m. And, finally, its magnitude could be estimated with fairly good accuracy by regarding the magnetized grains to be simple magnetic dipoles.

Acknowledgements

We are indebted to Professor S. García for his valuable comments and to J. López for assistance in computer programming.

References

1 **Kwastnitza, K., Jacob, B. and Vécsey, G.** Hysteretic effects in the flux-flow state of granular high-T_c superconductors *Physica C* (1990) **171** 211–215
2 **Evetts, J.E. and Glowacki, B.A.** Relation of critical current irreversibility to trapped flux and microstructure in polycrystalline $YBa_2Cu_3O_{7-\delta}$ *Cryogenics* (1988) **28** 641–649
3 **Chen, K.Y. and Quian, Y.J.** Critical current and magnetoresistance hysteresis in polycrystalline $YBa_2Cu_3O_{7-\delta}$ *Physica C* (1989) **159** 131–136
4 **Majoros, M., Polák, P., Stribik, V., Benacka, S. et al.** Hysteresis of transport critical currents in high temperature $YBa_2Cu_3O_{7-\delta}$ superconductors: bulk samples and thin films *Supercond Sci Technol* (1990) **3** 227–232
5 **Altshuler, E., García, S. and Aguilar, A.** Hysteretical critical currents in $YBa_2Cu_3O_{7-\delta}$ superconductors: a microstructural approach *Physica Stat Solidi (a)* (1990) **120** K169–K172
6 **Askew, T.R., Flippen, R.B., Leary, K.J. and Kunchur, M.N.** Local magnetic field distribution in polycrystalline $YBa_2Cu_3O_{7-\delta}$ and its influence on bulk critical currents *J Mater Res* (1991) **6** 1–13
7 **Navarro, R. and Campbell, L.J.** Intergranular fields and Josephson critical currents in HT_c ceramics *Supercond Sci Technol* (1992) **5** 100–105
8 **Peterson, R.L. and Ekin, J.W.** Josephson-junction model of critical current in granular $YBa_2Cu_3O_{7-\delta}$ superconductors *Phys Rev B* (1988) **37** 9848–9851
9 **Papa, A.R.R. and Altshuler, E.** $J_c(B)$ curves and the Josephson-junction assembly model in $YBa_2Cu_3O_{7-\delta}$ superconductors *Solid State Commun* (1990) **76** 799–801
10 **Senoussi, S., Hadjouji, S., Maury, R. and Fert, A.** Demagnetizing fields and other shape affects in high-T_c ceramics *Physica C* (1990) **165** 364–370
11 **Bean, Ch.P.** Magnetization of high-field superconductors *Rev Mod Phys* (Jan 1964) **36** 31–39
12 **Xu, M.** Critical current density and time-dependent magnetization of the high-transition temperature superconductors *PhD Thesis* Georgia Institute of Technology, USA (1990)
13 **Altshuler, E., García, S. and Barroso, J.** Flux trapping in $YBa_2Cu_3O_{7-\delta}$ superconductors: A fingerprint of intragrain properties *Physica C* (1991) **177** 61–66
14 **Vallet-Regi, M. and Gonzalez-Calbet, J.M.** Synthesis and microstructural characterisation of superconducting oxides, in: *Superconductivity in Spain: Research Activities in 1989* Programa Midas, Madrid, Spain (1990) 193
15 **Altshuler, E. et al.** *M vs. H* curves of granular superconductors, unpublished manuscript, Superconductivity Laboratory, University of Havana (1992)
16 **Clem, J.R.** Granular and superconducting-glass properties of high-T_c superconductors *Physica C* (1988) **153/155** 50–55
17 **Altshuler, E., Carrillo, D., Venegas, V., Papa, A.R.R. et al.** Anomalies in the J_c *vs B* curves for oxalate route Y-Ba-Cu-O superconductors *Physica C* (1990) **172** 361
18 **Purcell, E.M.** *Electricity and Magnetism* McGraw–Hill, New York, USA (1965)

Appendix: Estimation of G

Let us assume that the grains can be regarded as slabs of dimensions $a \times a \times c$, with $c > a$, surrounded by four 'junction layers' of area $a \times c$ and thickness δa, as represented in *Figure 6*. The grain magnetization provoked by the external field (applied along c) can be roughly represented by a magnetic dipole moment of magnitude $\boldsymbol{m} = \boldsymbol{M}(H_e, H_m)V$, where V is the volume of the grains. In such a case, we can take H_{gj} as the average of the z-component of the magnetic field over the junction volume associated with $\boldsymbol{m}$, which is given in Cartesian coordinates by

$$\langle H_z \rangle = \frac{\int H_z(x, y, z)\mathrm{d}V}{\int \mathrm{d}V} \qquad \text{(A1)}$$

where the integration takes place over the volume of the junction. It should be stressed that we have not considered any flux compression due to the presence of neighbouring grains. Inserting the expression for

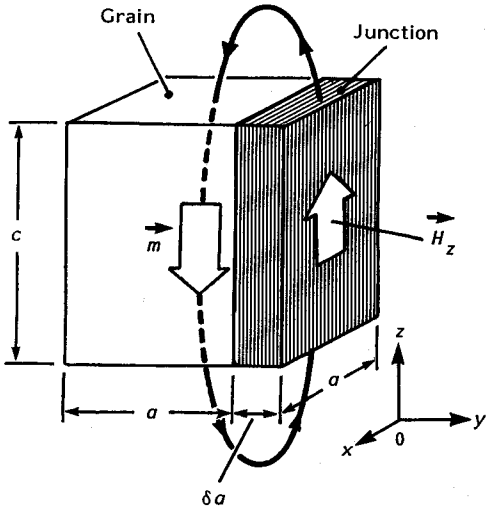

Figure 6 Assumed geometry for estimating the geometrical factor

$H_z = H_z(x, y, z)$ generated by a magnetic dipole[18] in (A1) and simplifying the integrals, we obtain

$$\langle H_z \rangle = M(H_e, H_m) \frac{a}{\delta a} \int_{-c/2}^{c/2} dz \int_{a/2}^{a/2+\delta a} dy \times \int_{-a/2}^{a/2} \frac{(2z^2 - x^2 - y^2)}{(x^2 + y^2 + z)^{5/2}} dx \qquad \text{(A2)}$$

We will define the geometrical factor related to an isolated grain, G', as the factor multiplying $M(H, H_m)$ in Equation (A2).

If we assign typical values of $a = 2$ μm, $c = 10$ μm (reference 5) and $\delta a = 0.4$ μm (reference 8), then $G' \approx 4 \times 10^{-2}$. Since it is clear that at least two grains contribute to the field on each junction, we can take $G \approx 2G'$, so the order of magnitude of G is 10^{-1}.

D.c. field tuning of inter- and intragranular effects in Y-Ba-Cu-O ceramics*

L.A. Angurel, F. Lera, C. Rillo and R. Navarro

Instituto de Ciencia de Materiales de Aragón, CSIC-Universidad de Zaragoza, Centro Politécnico Superior de Ingenieros, María de Luna 3, Zaragoza E-50015, Spain

The validity of critical state models (CSM) for the description of Y-Ba-Cu-O high temperature superconducting ceramics is checked at temperatures above that of liquid nitrogen. Isothermal magnetic a.c. susceptibility components at different excitation fields and in the presence of a d.c. tuning field, d.c. magnetization and critical current transport measurements are reported. Full analysis of all these data with the same set of CSM parameters leads to the derivation of the most adequate model for intergranular behaviour.

Keywords: high T_c superconductors; Y-Ba-Cu-O; critical state

The heterogeneous nature of ceramic high temperature superconductors (HTSC) strongly influences their magnetic and electric transport properties, and therefore their applications. Provided that at the temperatures of interest the penetration length, $\lambda(T)$, is much smaller than the average grain dimensions, two coexisting type II superconducting media may be considered: strong superconducting grains and a weak link network between them. Furthermore, when the differences in intensity of the inter- and intragranular superconducting properties are high enough, both effects may be experimentally separated. Thus at constant temperature the d.c. field may tune into one or the other effect.

Accordingly, analysis of both inter- and intragranular irreversible magnetic properties of HTSC ceramics may be performed using adequate critical state model (CSM) solutions[1,2] that take into account appropriate phenomenological field dependencies of the local critical current density. These include the potential model[3,4], where $J_c(H) = J_{c0}/|H|^n$, Kim's model[5,6], where $J_c(H) = (J_{c0}H_m)/(|H| + H_m)$; as well as a quadratic expression[7], where $J_c(H) = (J_{c0}H_m^2)/(|H|^2 + H_m^2)$; an exponential expression[8,9], where $J_c(H) = J_{c0}\exp(-|H|/H_m)$; and other generalized expressions[10,11], where $J_c(H) = (J_{c0}H_m^\beta)/(|H| + H_m)^\beta$ and H is the local field. In addition, in the study of intergranular properties, the heterogeneous nature of HTSC may be introduced by an effective permeability, μ_{cer}, which is a measure of the volume shielded by intragranular currents. In all these cases it is necessary to develop a method to fit the experimental data by obtaining a set of CSM parameters (J_{c0}, H_m, μ_{cer}, β) or (J_{c0g}, H_{mg}, β_g) that characterize the inter- or intragranular properties, respectively, of the sample at a given temperature.

In the analysis of the temperature variation of the magnetic and electric transport properties, the CSM characteristic parameters change through *a priori* unknown functions of T. Generally, satisfactory data fits are obtained but the CSM parameters, which are not easily verified experimentally, do not allow investigation of the different $J_c(H)$ dependencies. In a previous study[12], a method to obtain the intergranular CSM fitting parameters has been derived. As is well described in the literature[12,13] this method uses the height and position of the susceptibility's out-of-phase component maximum as a function of the a.c. field amplitude (h_0). Indeed, the maximum h_0 values generated by a particular apparatus limit the range of temperatures in which those fits are possible. This experiment, therefore, in most cases allows only the study of intergranular effects.

Up to now, most of the intergranular properties have been obtained from a.c. susceptibility measurements [$\chi(h_0)$], and intragranular effects have been studied using magnetization techniques. The superposition of a polarizing d.c. field (H_{dc}) parallel to h_0 and the measurement of $\chi(h_0, H_{dc})$ permit tuning into both contributions. In addition, at fixed temperatures, using different values of H_{dc} and h_0, the degrees of freedom in the CSM parameters may be reduced, and thus comparisons of the different models are possible.

In the present work different CSM predictions have been compared with appropriate measurements on a cylindrical Y-Ba-Cu-O ceramic sample. Both components of the a.c. susceptibility [$\chi'(h_0, H_{dc})$ and $\chi''(h_0, H_{dc})$] have been used, together with measurements of the a.c. susceptibility's third harmonic [$\chi_3(H_{dc})$], d.c. magnetization [$M(H_{dc})$] and transport critical current [$J_c(H_{dc})$], performed at 83 K. Theoretical predictions of $\chi(h_0, H_{dc})$, $\chi_3(H_{dc})$ and $M(H_{dc})$ have been derived to analyse the differences

* Paper presented at the conference 'Critical Currents in High T_c Superconductors', 22–24 April 1992, Vienna, Austria

0011–2275/93/030314–07